CHINESE JOURNAL OF MECHANICAL ENGINEERING
Vol. 26, No. 6, 2013

DOI: 10.3901/CJME.2013.06.1204, available online at www.springerlink.com; www.cjmenet.com; www.cjmenet.com.cn

Detecting the Position of the Moving-iron Solenoid by Non-displacement Sensor Based on Parameter Identification of Flux Linkage Characteristics

WANG Xuping, QUAN Long*, and XIONG Guangyu

Key Laboratory of Advanced Transducers and Intelligent Control System of Ministry of Education, Taiyuan University of Technology, Taiyuan 030024, China

Received September 6, 2012; revised August 16, 2013; accepted August 28, 2013

Abstract: Currently, most researches use signals, such as the coil current or voltage of solenoid, to identify parameters; typically, parameter identification method based on variation rate of coil current is applied for position estimation. The problem exists in these researches that the detected signals are prone to interference and difficult to obtain. This paper proposes a new method for detecting the core position by using flux characteristic quantity, which adds a new group of secondary winding to the coil of the ordinary switching electromagnet. On the basis of electromagnetic coupling theory analysis and simulation research of the magnetic field regarding the primary and secondary winding coils, and in accordance with the fact that under PWM control mode varying core position and operating current of windings produce different characteristic of flux increment of the secondary winding. The flux increment of the electromagnet winding can be obtained by conducting time domain integration for the induced voltage signal of the extracted secondary winding, and the core position from the two-dimensional fitting curve of the operating winding current and flux-linkage characteristic quantity of solenoid are calculated. The detecting and testing system of solenoid core position is developed based on the theoretical research. The testing results show that the flux characteristic quantity of switching electromagnet magnetic circuit is able to effectively show the core position and thus to accomplish the non-displacement transducer detection of the said core position of the switching electromagnet. This paper proposes a new method for detecting the core position by using flux characteristic quantity, which provides a new theory and method for switch solenoid to control the proportional valve.

Key words: switch solenoid, flux characteristic quantity, position detection, non-displacement sensor

1 Introduction

Electromagnet is an important component of electro-hydraulic control valve used for converting the input electric signals to mechanical output. Therefore, the performance of solenoid will directly influence the functionality of the hydraulic valve. Usually there are two kinds of solenoids for driving the electro-hydraulic valve, respectively, switching type and proportional type;while according to the structural forms we have moving-iron, moving-coil, and step-type electro-mechanical converters. The moving-iron switching solenoid features simple structure and low cost, but it has only ON and OFF positions and is mainly used to control the switching valve; the moving-iron proportional solenoid, thanks to the specially-design of isolated magnet ring structure, is provided with horizontal output characteristic and used to control proportional valves and servo proportional valve. The proportional valve can also be driven by stepper motors, moving-coil solenoids and other electro-mechanical converters. Compared to switch solenoid valves, the proportional solenoid valve has a more complicated structure and higher cost[1–3]. Hence, to enable the switch solenoid valve with proportional output force characteristic will have a significant effect in reducing the cost of electro-hydraulic proportional valve and simplifying its structure. Many native and foreign researchers have done a lot of research works. Some documents have theoretically analyzed the feasibility of feature of electromagnetic quasi-steady force by considering optimized electromagnetic structural processing and magnetic path. Refs. [4–6] conduct researches from different aspects, e.g., optimize the performance of magnetic circuit by improving the structure of switch solenoid, and thus promote the force characteristics of switch solenoids; or compensate output electromagnetic force by real-time detection of the moving-iron position with a displacement sensor[7–8]. Many of the domestic and foreign researches have tried to accomplish parameter identification of model with current and voltage signals in order to monitor the output force, displacement or speed of the solenoid[9–11].

When a solenoid is driving the hydraulic valve, as fluid flows through the valve core, the surroundings are totally sealed and there is no extra space available in the solenoid

* Corresponding author. E-mail: quanlong@tyut.edu.cn
This project is supported by National Natural Science Foundation of China(Grant No. 51175362)

for installing the displacement sensor, what's more the displacement sensor can be expensive and difficult to install, hence, how to achieve proportional control by using low-cost and simple switch solenoid without displacement sensor has become the focus of research for many scholars recently. For example, LIM, et al[12], and RAHMAN, et al[13–14], from University of New South Wales carried out researches on detection of non-displacement sensor of the moving-iron position of the switch solenoid, and finally achieved the non-displacement sensor detection of the moving-iron position by using certain algorithm and special hardware circuit according to the relationships between winding incremental inductance, moving iron location and current of the switch solenoid; however, as the current rate of change is small and the signals are subject to temperature change, it is difficult to obtain the detecting signals, which is of a great concern.

To address the problem in the said position detection method of non-displacement sensor, according to the electromagnetic coupling principle, a new method is put forward by adding one more set of secondary winding for moving-iron position detection on the basis of a common switching electromagnet. The original power winding of the solenoid and the extra secondary winding respectively serves as working winding and measuring winding. The moving-iron position is detected by extracting the flux linkage characteristic quantity via the measuring winding. Hence, a new theory and method is proposed for control of the proportional valve by a switch solenoid.

2 Rules for Detecting the Positions of Switching Electromagnet

The structure of switching electromagnet is, shown as Fig. 1, composed of an armature, a guide sleeve and two windings (the primary winding serves as the working winding, and the secondary as measuring winding), a shell and a pull rod.

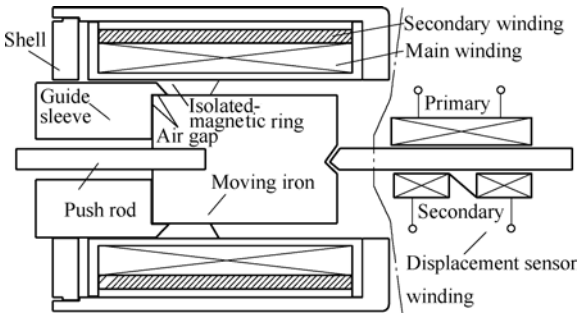

Fig. 1. Schematic diagram of switching electromagnet structure

The guide sleeves acts as high-pressure resistance and serves as part of the magnetic circuit, the front and the rear sections thereof are made of magnetic materials, and the middle section is made of non-magnetic materials (the isolated–magnetic ring) and other devices for protecting coils. The right side of Fig. 1 presents the position sensor used for measuring the displacement when the solenoid serves as the hydraulic valve actuator, which is mechanically connected with the solenoid. The shadow part indicates the secondary winding additionally arranged for detecting the moving-iron position of the solenoid.

The relationship between the primary and secondary windings of the switching electromagnet is shown in Fig. 2. Where, R_1 and R_2 represent respectively the resistance of the primary and the secondary windings, L_1 and L_2 refer to the inductance parameter of the two windings, and M refers to the mutual inductance parameter of the primary and secondary windings.

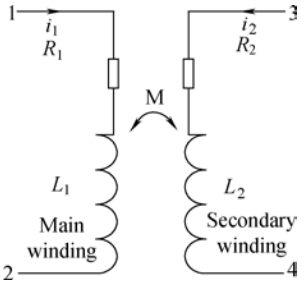

Fig. 2. Schematic diagram of solenoids of the primary and the secondary windings

According to the electromagnetic theory, the primary winding is applied with voltage, and the secondary winding is open circuited, the formula for secondary winding terminal voltage can be derived as Eq. (1):

$$u = \frac{\mathrm{d}\psi(x,i)}{\mathrm{d}t} = M(x,i)\frac{\mathrm{d}i}{\mathrm{d}t} + i\frac{\partial M(x,i)}{\partial x}v, \tag{1}$$

where u_2, i_1, x and ψ refer to the secondary winding terminal voltage, the primary winding current (the current is 0 A where the secondary winding is open circuited), moving-iron position and the secondary winding flux; M represents the mutual inductance between the primary and secondary windings; v represents the moving-iron speed. $M(x,i)\,\mathrm{d}i/\mathrm{d}t$ means the transformer potential while $iv\partial M(x,i)/\partial x$ means the motion potential.

As seen from Eq. (1), the secondary winding terminal voltage is associated with the moving-iron position, the primary winding current and current change rate and the moving-iron speed. Eq. (2) can be obtained from

$$\begin{cases} u = \dfrac{\mathrm{d}\psi(x,i)}{\mathrm{d}t}, \\ \psi(x,i) = \int u\mathrm{d}t. \end{cases} \tag{2}$$

Eq. (2) is the theoretical base for measurement of the secondary winding flux linkage, which is only dependent on the current of the primary winding if the displacement is given. This measuring method merely involves

measurement of the secondary winding terminal voltage u_2, and the current of the primary winding i_1, disregarding either influence of motion potential or u_1-R_1i_1, As the secondary winding flux is only related to the moving-iron position and the current of the primary winding, we can work out the winding flux according to the voltage and current, and the relation curve of the three items can be obtained from the characteristic test of switching electromagnet winding flux. If x is given, the secondary winding flux $\psi(x, i_1)$ is only related to the current i_1. When the magnetic circuit is not highly saturated, x can be estimated through using $\psi(x, i_1)$ and i_1, i.e.,

$$x = f(\psi(x, i), i). \tag{3}$$

The flux characteristic curve of the secondary winding is shown in Fig. 3. When the current of the primary winding changes from i_n to i_{n+1}, due to the varying gradient of each flux current curve at different location, the flux variation $\Delta\psi$ (namely, flux characteristic quantity G) may vary accordingly.

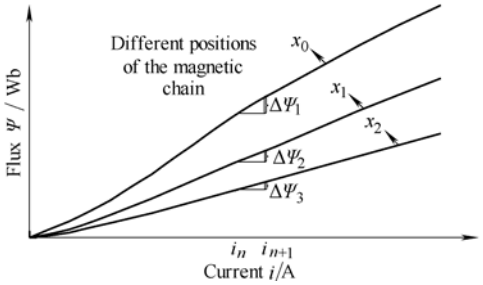

Fig. 3. Flux linkage versus current

Hence, theoretically, we can use the voltage of the secondary winding u_2 to calculate the flux increment of the secondary winding and use relevant current to estimate the moving-iron position.

Eq. (3) is the theoretical base of displacement identification and estimation. Under PWM control mode, the primary winding current i_1 and the secondary winding u_2 can be measured, whose wave form is shown in Fig. 4. When the moving-iron moves, as mechanical inertia is way greater than the electromagnetic time constant[14], in the interval t_N−t_{N+1}, the displacement can't change in time, and the flux variation of the secondary winding $\Delta\psi$ (i.e., flux characteristic quality G) in this time period can be calculated from the Eq. (4) below:

$$G(x, i_N, i_{N+1}) = \int_{t_N}^{t_{N+1}} u_2(t)\mathrm{d}t, \tag{4}$$

where, the flux characteristic quantity can be obtained by measuring u_2 and the corresponding i_1 and applying digital integration for u_2, According to the calculated flux characteristic quantity and the primary winding current, the estimation of the moving-iron position can be achieved.

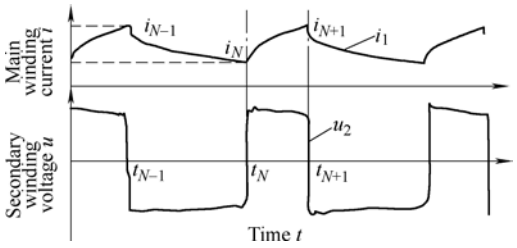

Fig. 4. Illustration of flux characteristic quantity of the secondary winding

3 Winding Flux Characteristic of Switching Solenoid

To use the above-mentioned method, it is necessary to measure the flux of the secondary winding. The switching electromagnet with 1 A rated current is used in the research, and a secondary winding for displacement detection is also provided as prototype for actual calculation. Magnetic circuit of the device is shown in Fig. 5, where the circuit is divided into ϕ_1 and ϕ_2 at the vicinity of the main gap. The main magnetic circuit ϕ_1 gets access to the armature from the bottom of the basin-shaped pole shoe by passing through the working gap axially; the magnetic circuit ϕ_2 gets access to the armature from peripheries of the basin-shaped pole (the front section of the guide sleeve) by passing through the radial gap, and then converges with some ϕ_1.The finite element analysis software Ansoft and electromagnetic finite mesh division are applied to analyze and calculate the two-dimensional field, as shown in Fig. 6. Due to presence of the copper ring, the guide sleeve and the pole shoe are combined to form a basin-shaped pole shoe with a tapered end, it seems like adding a sub magnetic circuit in the working gap area.

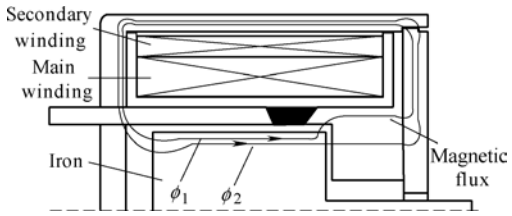

Fig. 5. Schematic diagram of solenoid magnetic lines

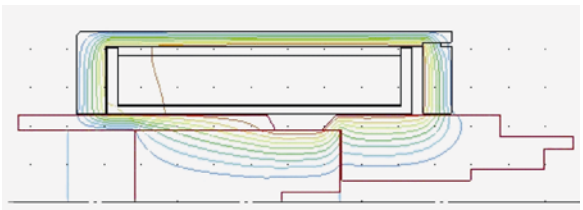

Fig. 6. Two-dimensional magnetic field distribution of solenoid

Due to the distribution of magnetic parameters and the nonlinear magnetization characteristics, the traditional computational analysis on static characteristics of the electro-mechanical converters is rather complicated. From

the magnetic field distribution, switch magnetic has uneven distribution of the magnet fields and local saturation phenomena. Its electromagnetic properties can be described by motor magnetization curve family which shows the relationship between the motor winding flux, the relative position of the moving-stator and the current, i.e., the $\psi(x, i)$ curve. The curve will give a direct affect on the motor analysis, design and control, and in case of magnetic circuit saturation, to ensure accurate calculation of the $\psi(x, i)$ curve, it is necessary to create an accurate electromagnetic mathematical model and establish a correct electromagnetic mathematical model, including magnetic characteristics, static force characteristics, etc. The electromagnetic mathematical model can be obtained by two methods, namely the finite element method and the measurement method[15]. In this paper, the test measurement method is applied to measure the static electromagnetic properties of the switching electromagnet.

The flux of the test circuit is shown in Fig. 7, where a digital acquisition instrument is used to record the secondary winding voltage and the primary winding current during discharging of the primary winding. The winding flux is indirectly calculated from the coil current and the coil voltage detected through the sample resistance.

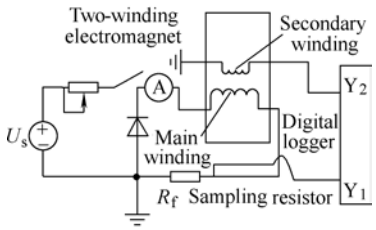

Fig. 7. Flux test circuit

Apply DC voltage to the primary winding and open circuit of the secondary winding according to the following principle for testing flux characteristic of secondary winding. According to the electromagnetic theory, the secondary winding terminal voltage shall comply with Eq. (2). The manual adjustment mechanism in the test system is used to fix the position of the moving-iron to make $x=x_0$. Waveforms for the secondary winding induced voltage measured at each fixed position and the corresponding current of the primary winding are shown in Fig. 8.

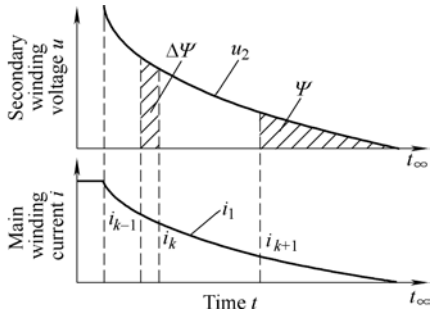

Fig. 8. Voltage response of secondary winding ($x=x_0$)

In Fig. 8, t_∞ corresponds to the moment of discharging completion of the primary winding discharge (the current is 0 A). Where ψ refers to the flux of the secondary winding when the primary winding current range from 0 to i_{k+1}; while $\Delta\psi$ refers to the flux change when the primary winding current changes from i_{k-1} to i_k. It can be seen that the variation of flux ψ at different currents differs from the variation of flux $\Delta\psi$ at different current change interval.

The flux, current and displacement curve obtained from test is shown in Figs. 9(a), 9(b) and 9(c). Fig. 9(c) is a three-dimensional graph when the flux changes with the current and the displacement. As can be seen from Fig. 9(a) curve of flux changes with displacement at different currents and Fig. 9(b) curve of flux change with current under different displacements, the flux changes with the change of magnetic resistance (i.e., the moving-iron position) and current value.

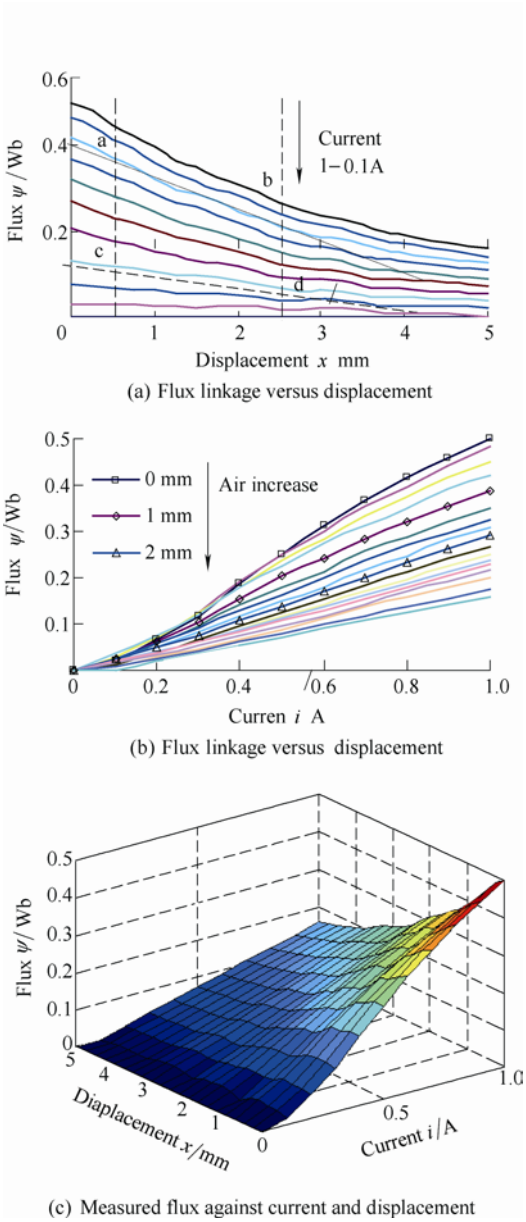

Fig. 9. Relation curve of flux, displacement and current of the switching solenoid

It can be drawn from theoretical analysis and test results, where the magnetic circuit is not highly saturated and the supply current of the winding is not so small, the curves shown in Fig. 9(b) will not overlap or intersect with each other, so it is possible to detect the moving-iron position from the secondary winding flux within the effective range.

As shown in Fig. 9(a), the electromagnetic force and flux produced are relatively small when the current is within (0–0.2 A); when the gap is greater than 2.5 mm, the flux change caused by magnetic resistance will hardly be shown; the magnetic circuit can be slightly saturated where the gap is small and the current is greater than 0.8 A. Therefore, the range of estimated position is within the interval included by a, b, c, and d straight lines shown in Fig. 9(a).

4 Position Detection of the Switching Solenoid

In order to achieve position identification and estimation of the switching solenoid, a proportional amplifier PWM is adopted to control the solenoid, and the moving-iron position may be detected by the flux characteristics quantity that can identify positions and is extracted by induced voltage signal of the secondary winding side.

4.1 Winding current and flux characteristics under the PWM Mode

As a moving-iron switching electromagnet for driving the switching valve, the proportional amplifier adopts pulse width modulation (PWM). Schematic diagram of PWM control amplifier for primary and secondary windings of the switching electromagnet is given in Fig. 10.

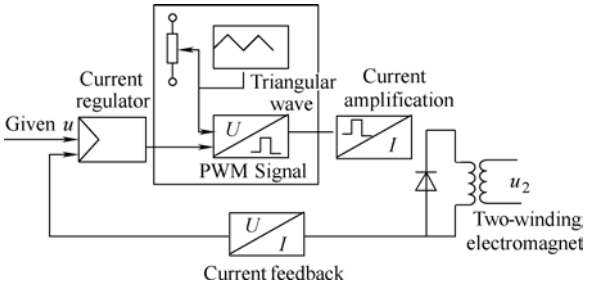

Fig. 10. PWM control principle of the primary and secondary windings of the solenoid

It is composed of a pulse width modulator, a current regulator, current feedback and a power driver circuit. Voltage/current proportion circuit may drive the switching solenoid and the control principle applies current closed-loop feedback. Certain voltage signal is input signal to the proportional amplifier and the average current of the primary winding coil of the switching electromagnet shall be the corresponding proportional current value.

Under PWM control model, current waveform of the primary winding and the induced voltage waveform of the secondary winding are shown in Fig. 11, and the secondary windings induced voltage waveform is close to a square wave.

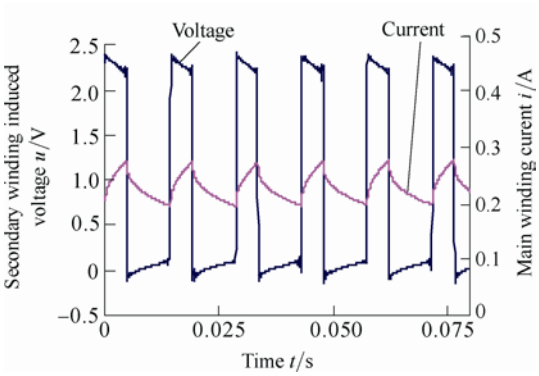

Fig. 11. Current of the primary winding and the induced voltage of the secondary winding

The induced voltage of the secondary winding is also different when the supply current of the primary winding varies. Fig. 12 shows the test waveform of the induced voltage of the secondary winding when the current is the same, while the iron is under different displacements. It can be learned from the figure and the previous theoretical analysis that, when different currents are applied for the primary winding, given the different moving-iron positions, the induced voltage of the secondary winding may vary. The flux characteristics quantities $G(x, i_1)$ obtained from voltage integration of the secondary winding will also change with the moving-iron position and the winding current. Experimental results show that the variation range of flux characteristic is about 20 mv, when moving iron in different locations and working current at the same current.

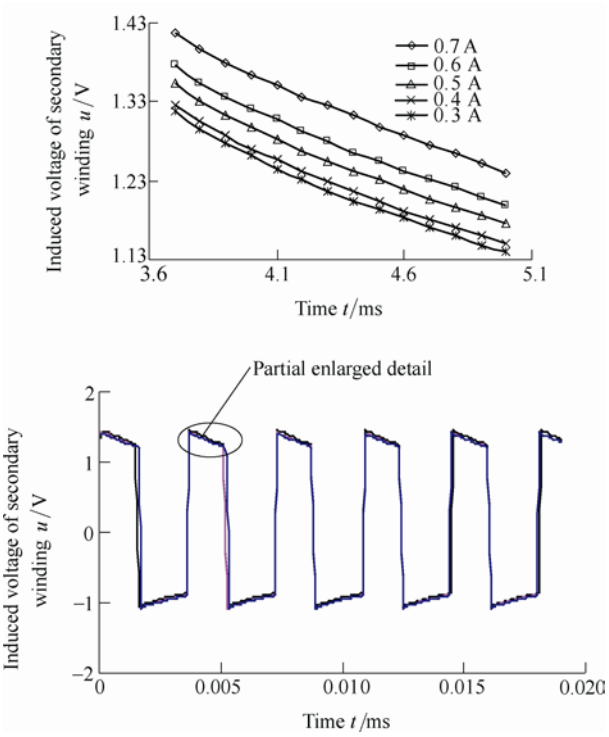

Fig. 12. Induced voltage of the secondary winding at different positions

4.2 Band-stop filter of the interference signal

In the testing process, the low-frequency interference signal generated by the electric circuit of the proportional

amplifier is coupled to the secondary winding side, so there is low-frequency interference signal in voltage signal induced at the secondary winding side, as shown in Fig. 13(a), the interference frequency is around 7.2 Hz. Hence, Butterworth band-stop filter is used for solving the interference signal of secondary winding voltage. After filtering with the band-stop filter, the signals of voltage induced at the secondary winding side are shown in Fig. 13(b).

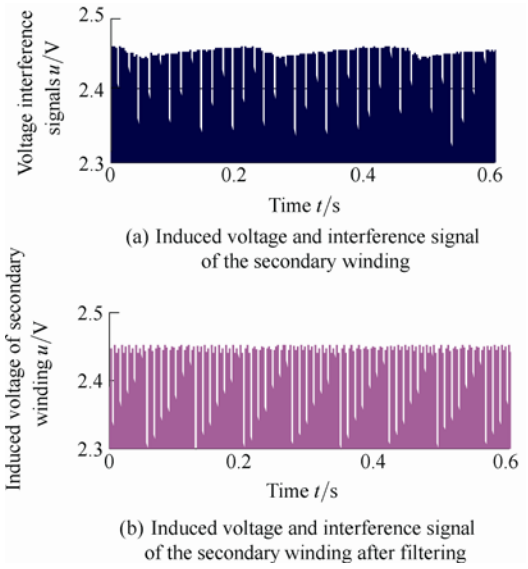

Fig. 13. Voltage signal of the secondary winding before and after filtering

Fig. 14 shows the comparison of flux characteristic quantity extracted from the secondary winding before and after filtering given the same supply current and the identical moving-iron position (1.75 mm), it can be seen that the low-frequency interference is greatly reduced after filtering.

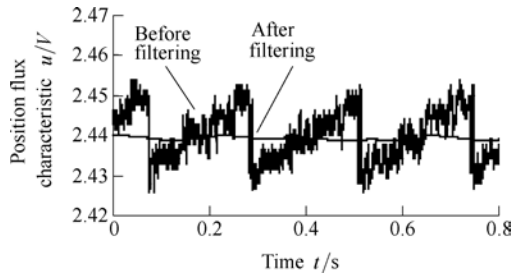

Fig. 14. Flux characteristic quantity and the interference signal contained x=1.75 mm, i_1=0.7 A

5 Test Verification

Fig. 15 is the schematic diagram of dynamic and static tests for switching electromagnet position estimation, manual mechanical feeding experiment mechanism shown in Fig. 15 is used as the displacement feed mechanism for the static test; the spring or the connection rod is used to connect the auxiliary system and EMT (rod for static test and spring for dynamic test). Where the primary winding coil current and the measured flux characteristics of the secondary winding as well as the position of the moving-iron are applied for curve fitting, the position identification and detection of the moving-iron can be achieved. Computer is used for control and management of the test system, and DSpace RTC is the real-time control card dedicated to real-time simulation test.

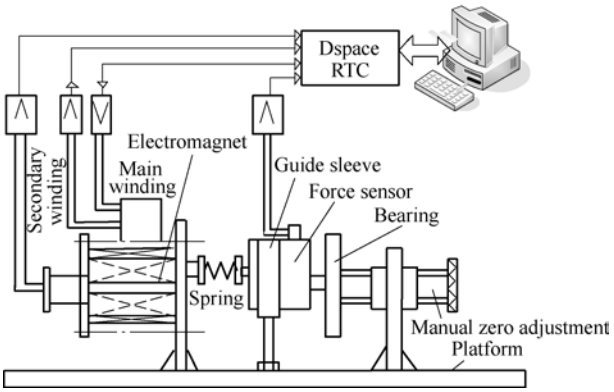

Fig. 15. Experimental set-up of the position identification and estimation of switching solenoid

Calculation of the flux characteristics which reflects the displacement change is not confined to a small area of t_{N-1}−t_N shown in Fig. 4. It can also use t_N−t_{N+1} interval to carry on integral calculation (Select larger value area) or use the average value of several intervals to reduce the error.

Table 1 shows the actually flux characteristic quantity measured with supply current increasing when the two-winding switching electromagnet are controlled at different positions.

Table 1. Position flux characteristic of the secondary winding when the current rise Wb

Position	Current i/A				
x/mm	0.3	0.4	0.5	0.6	0.7
0	1.010	1.802	3.384	5.565	7.814
0.25	1.389	2.533	4.182	6.142	8.372
0.50	1.589	2.952	4.863	6.933	9.554
0.75	1.939	3.251	5.405	7.401	10.534
1	2.440	3.832	6.174	7.831	11.562
1.25	2.492	4.105	6.682	8.470	12.533
1.50	2.872	4.738	7.131	9.014	13.232
1.75	3.093	4.967	7.910	9.778	14.201
2	3.245	5.338	8.201	10.544	14.945

Table 2 shows the flux characteristic quantity measured when the supply current drops with the switching electromagnet at different positions (hysteresis may occur due to hysteresis effect, but neither is within the magnetic saturation range). But the hysteresis between two tables is not practical sense hysteresis. Fig. 16 gives the fitting curve of the flux characteristic quantity and moving-iron position

at different currents (with current rising). The flux increment calculated and tested according to the flux increment theory proves the accuracy of the data in Tables 1 and 2.

Table 2. Position flux characteristic of the secondary winding when current decline Wb

Position	Current i/A				
x/mm	0.3	0.4	0.5	0.6	0.7
0	2.450	3.350	4.430	7.440	10.800
0.25	2.821	4.003	4.914	7.814	11.212
0.50	3.002	4.611	5.851	8.342	11.561
0.75	3.351	4.935	6.612	8.483	12.245
1	3.855	5.484	6.932	9.091	12.817
1.25	3.958	6.003	7.533	9.232	13.215
1.50	4.303	6.391	8.096	9.921	14.163
1.75	4.521	6.562	8.748	10.511	14.621
2	4.672	7.142	9.027	10.911	15.034

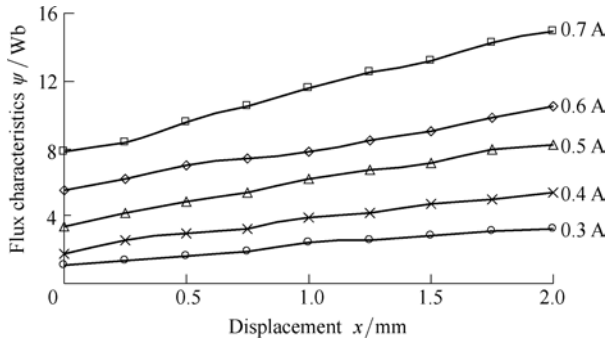

Fig. 16. Fitting curve of the position of characteristic quantities

Fig. 17 is the estimation curve of displacement under manual feed. It can be learned that the estimated curve is basically consistent with the actual curve. Fig. 18 shows the fixed position of moving-iron, displacement estimation curve and the corresponding magnetic force waveform at an input current of 0.3 A and 0.7 A. From the figures, we can get the displacement delay electromagnetic force of the moving-iron. When the input current is 0.3 A, it takes longer to reach the designated position. The response time may vary under different given input valves.

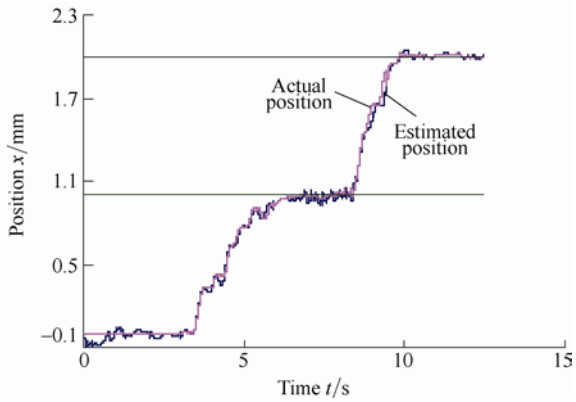

Fig. 17. Manual feed position estimation curve

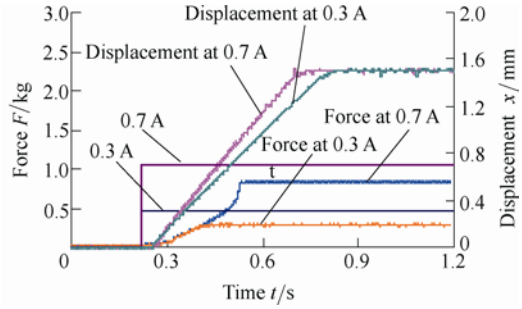

Fig. 18. Test results of displacement estimation at different steps

Fig. 19 is the displacement estimation curve obtained from the test with input triangular wave current being within 0.3–0.6 A. The interference signals are mainly concentrated at places where the displacement is relatively small, i.e., the u_2 value is relatively small. The estimation error of x in the actual results depends on the measurement precision and calculating accuracy of $G(x, i_1)$, i_1 and u_2. Small u_2 will lead to increased measurement error, which can be solved by increasing the number of turns of secondary windings.

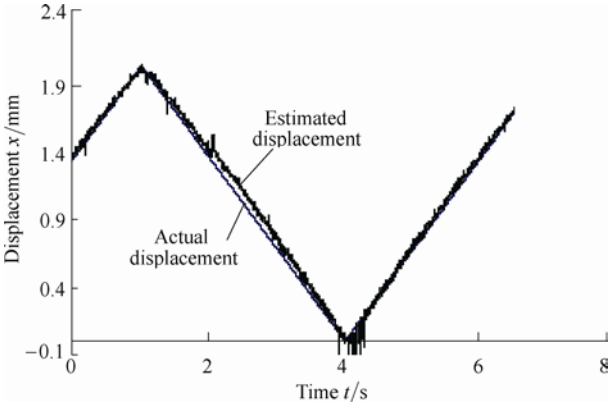

Fig. 19. Estimated position of the moving-iron i_1=0.6 A while tracking the given triangle wave

6 Conclusions

(1) Through the electromagnetic theory of switching electromagnet and the process analysis of the dynamic model, the experimental method is applied to measure the static electromagnetic properties of the switching electromagnet and acquire the electromagnetic mathematical model of the solenoid.

(2) By extracting the flux characteristic obtained by integration of secondary winding voltage signals, the relations between the moving-iron, the coil current and the flux characteristic quantity are identified.

(3) Curve fitting of the flux characteristic quantity of the secondary winding, primary winding current and the position of the moving-iron in detecting the position of the solenoid is of great significance in deciding the reliable action of the valve core. It provides a new idea for using switching electromagnet to control proportional valve.

References

[1] WANG Shuhong, XIONG Guangyu. Analysis of air-gap field in a new tubular linear PM motor with moving coil[J]. *Transactions of China Electrotechnical Society*, 2007, 22(5): 40–44.

[2] XU Xiaoqing, QUAN Long, WANG Xuping. Principle and characteristics of novel 2-degree-of-freedom electro-mechanical transformers used in valves[J]. *Proceedings of the CSEE*, 2010, 30(3): 119–123.

[3] SHI Shengjun, CHEN Weishan, LIU Junkao, et al. Ultrasonic linear motor using longitudinal and bending multimode bolt-clamped langevin type transducer[J]. *Proceedings of the CSEE*, 2007, 27(18): 30–34. (in Chinese)

[4] WANG Shuhong, XIAO Xuliang, XIONG Guangyu. Direct current electromagnets with constant traction characteristic[J]. *Chinese Journal of Mechanical Engineering*, 2008, 44(2): 244–247.

[5] CHEN Youping, DU Zhiqiang, AI Wu, et al. Research on model of a new short-stroke linear motor and its experiments[J]. *Proceedings of the CSEE*, 2005, 25(7): 131–136. (in Chinese)

[6] ZENG Lingquan, KANO Yoshio, MA Hongru Imorove. Thrust characteristic of linear electromagnetic solenoid[J]. *Journal of Northeast Dianli University*, 1997, 17(1): 12–17. (in Chinese)

[7] XU Xiaoqing, QUAN Long, LI Bin. Study on controlling theories and methods of switching solenoids proportional servo valve[J]. *Proceedings of the CSEE*, 2009, 29(21): 93–98.

[8] WANG Xuping, QUAN Long, XU Xiaoqing. Principle and method for improving the switch solenoid characteristics with signal compensator[J]. *Proceedings of the CSEE*, 2010, 30(27): 117–122.

[9] ESPINOSA A G, RUIZ J R R, CUSIDO J, et al. Sensorless control and fault diagnosis of electromechanical contactors[J]. *Industrial Electronics, IEEE Transactions on*, 2008, 55(10): 3 742–3 750.

[10] RENN J C, CHOU Y S. Sensorless plunger position control for a switching solenoid[J]. *JSME International Journal Series C*, 2004, 47(2): 637–645.

[11] ESPINOSA A G, RUIZ J R R, MORERA X A. A sensorless method for controlling the closure of a contactor[J]. *Magnetics, IEEE Transactions on*, 2007, 43(10): 3 896–3 903.

[12] LIM K W, CHEUNG N C, RAHMAN M F. Proportional control of a solenoid actuator[C]//*Industrial Electronics, Control and Instrumentation*, Sep. 5–9 1994, Bologna, Italy, IECON'94, 1994, 3: 2 045–2 050.

[13] RAHMAN M F, CHEUNG N C, LIM K W. Position estimation in solenoid actuators[J]. *Industry Applications, IEEE Transactions on*, 1996, 32(3): 552–559.

[14] RAHMAN M F, CHEUNG N C, LIM K W. A sensorless position estimator for a nonlinear solenoid actuator[C]//*Industrial Electronics, Control, and Instrumentation*, Nov. 6–10, 1995, Orlando, FL, 1995, 2: 1 208–1 213.

[15] QU Bingni, SONG Jiancheng, ZHANG Hongda, et al. Experimental research on mutual inductance in switched reluctance motor operated in two-phase excitation model[J]. *Transactions of China Electrotechnical Society*, 2010, 25(3): 33–39.

Biographical notes

WANG Xuping, female, born in 1976, is currently a PhD candidate at *Taiyuan University of Technology, China*. His research interests include the electro-hydraulic servo system components, control theory and methods.
Tel: +86-13485339796; E-mail: wxpxue@126.com

QUAN Long, male, born in 1959, is currently a professor and a PhD candidate supervisor at *Taiyuan University of Technology, China*. His research interests include mechatronics engineering, fluid power transmission and control.
Tel: +86-15333683330; E-mail: quanlong@tyut.edu.cn

XIONG Guangyu, male, born in 1946, is currently a professor and a PhD candidate supervisor at *Taiyuan University of Technology, China*. His research interests include the special motor.
E-mail: xiongguangyu@tyut.edu.cn